



Heteroclinic Cycles in a Competitive Network

Ulises Chialva

*CONICET, Departamento de Matemática,
 Universidad Nacional del Sur, Av. Alem 1253,
 8000 Bahía Blanca, Buenos Aires, Argentina
 uchialva@gmail.com*

Walter Reartes

*Departamento de Matemática,
 Universidad Nacional del Sur, Av. Alem 1253,
 8000 Bahía Blanca, Buenos Aires, Argentina
 walter.reartes@gmail.com*

Received September 6, 2017

The competitive threshold linear networks have been recently developed and are typical examples of nonsmooth systems that can be easily constructed. Due to their flexibility for manipulation, they are used in several applications, but their dynamics (both local and global) are not completely understood. In this work, we take some recently developed threshold systems and by a simple modification in the parameter space, we obtain new global dynamic behavior. Heteroclinic cycles and other remarkable scenarios of global bifurcation are reported.

Keywords: Competitive networks; heteroclinic cycles; global bifurcations; nonsmooth systems.

1. Introduction	2
2. Preliminaries	2
3. The Modified Case	3
3.1. The limit cycle	4
3.2. The heteroclinic cycles	4
3.2.1. Connections of eq_i with eq_{ki}	4
3.2.2. Connections of eq_0 with eq_i	5
3.2.3. The other connections	6
3.2.4. The twisting effect	6
3.3. Analysis of saddle connections	8
3.3.1. Connection between eq_i and eq_{ji}	8
3.3.2. Heteroclinic and homoclinic bifurcations	11
3.4. The main result	13
3.4.1. The q_α^i family	14
4. The Coloring Phenomena	15
References	16

1. Introduction

Competitive networks essentially consist of nodes and its interactions [Hirsch, 1982]. Due to the ease of building them, competitive networks are used as models in several disciplines as neuroscience, economy and ecology [Grossberg, 1988; Allesina & Levine, 2011; Levine *et al.*, 2017; Rondelez, 2012; Hopfield, 1982; Itskov *et al.*, 2011]. A way to build them is to assign a system of differential equations to a directed graph. While the graph represents the architecture of the network, the solutions of the new associated system represent activity measures of nodes.

A competitive threshold linear network (CTLN) is a special case of competitive network where the associated system is piecewise linear [di Bernardo *et al.*, 2008; Simpson, 2010]. Several systems of this type were widely studied for concrete and some restrictive cases in [Tang *et al.*, 2005; Hahnloser, 1998; Hahnloser *et al.*, 2003; Curto *et al.*, 2012, 2013; Curto & Morrison, 2016; Morrison *et al.*, 2016]. In those articles the *emergent dynamic* for simple cases was exhibited, showing a rich and fundamentally nonlinear behavior, such as multistability, periodic attractors, and chaos [Snoussi, 1989; Dai, 2008; di Marco *et al.*, 2000]. These types of competitive network models are recent examples of traditional analyses based on just asymptotic results of behavior as time goes to infinity. For example, in the traditional applications of CTLNs such as the one developed in [Curto *et al.*, 2012] (refer to the *Network Encoding Problem* [Amit, 1989]) or [Hahnloser *et al.*, 2003], the inputs are coded as *permitted sets*, i.e. as Boolean vectors that represent the support of some asymptotic stable equilibrium. On the other hand, in [Parmelee, 2016] they try to decode the patterns that arise as sequences of maximum of those stable limit cycles produced by the network. However, as we show in this paper, such competitive networks may also exhibit relevant scenarios for modeling transient behavior, analogous to those described in [Rabinovich *et al.*, 2001; Rabinovich *et al.*, 2008; Muezzinoglu *et al.*, 2009; Rabinovich *et al.*, 2014]. In such works, heteroclinic cycles produced by nonsymmetric connectivity networks are of fundamental importance in order to encode inputs as patterns generated by a transient trajectory.

In this work, we modify the weights of inhibitions between nodes and introduce new parameters on nonsymmetric systems already studied in

[Morrison *et al.*, 2016] to obtain new global dynamic behaviors not reported yet (like heteroclinic connections and heteroclinic cycles). In particular, a wide variety of heteroclinic cycles are described, especially those involving saddle equilibria, given their importance in modeling competitive phenomena such as those mentioned in [Muezzinoglu *et al.*, 2009]. Also, we found almost-chaotic behaviors such as cascades of bifurcations, homoclinic connections and finally we report a strange phenomena obtained by coloring some heteroclinic trajectories. In the first section we introduce the definitions for CTLNs and commonly-used notations of the principal previous works, and expose the necessary basic results to study those systems. The second part is dedicated to describe the basic behavior of a new piecewise linear system obtained from modifying an older model presented in [Morrison *et al.*, 2016]. In the next two sections we expose, by simulation, a global bifurcation that consists in the disappearance of a limit cycle and the appearance of heteroclinic cycles and we give a proof of the existence and appearance of some connections involving saddle equilibria. The last section is dedicated to report the strange coloring effect obtained from simulation and we conjecture some facts from it.

2. Preliminaries

Consider the n -dimensional *threshold linear network* represented by the equations

$$\dot{x}_i = -x_i + \left[\sum_{j=1}^n W_{ij} x_j + b_i \right]_+ . \quad (1)$$

According to the notation established in [Curto *et al.*, 2012, 2013; Morrison *et al.*, 2016], we call W the connectivity matrix and write W_i for its i th row. The vector $b \in \mathbb{R}^n$ is the denominated *input* of the system (1), and the function $[\cdot]_+$ is defined by $[y]_+ = \max\{0, y\}$. A *competitive threshold linear network (CTLN)* is a special case of (1) where $W_{ii} = 0$ and $W_{ij} < 0$. Each dynamical variable of system (1) represents the measure of activity of some node, and the value of the ij -entries describes the influence of j -node over the i -node. We label as *inhibitory* those connections with $W_{ij} < 0$. The self-inhibition (or decay rate) of a single node, which has been normalized to -1 , provides a natural scale for classifying the inhibition (cf. [Morrison *et al.*, 2016]). Given a connection with origin

on j -node and end on i -node, we call it *strong* if $W_{ij} < -1$ (i.e. the inhibition of j -node over i -node is higher than the self-inhibition of i -node), and *weak* if $W_{ij} > -1$ (the opposite inhibitory scenario). Also, we consider the functions f_i defined by

$$f_i(x) := \sum_{j=1}^n W_{ij}x_j + b_i. \tag{2}$$

Given a subset $\sigma \subset \{1, \dots, n\}$ we call

$$S_\sigma = \{x \in \mathbb{R}^n : f_i(x) < 0 \Leftrightarrow i \in \sigma\}. \tag{3}$$

At the same time, we write

$$\begin{aligned} S_0 &= \{x \in \mathbb{R}^n : \forall i f_i(x) > 0\} \quad \text{and} \\ S_- &= \{x \in \mathbb{R}^n : \forall i f_i(x) \leq 0\}. \end{aligned} \tag{4}$$

Finally, the *transition varieties* are defined as follows

$$\Sigma_i = \{x \in \mathbb{R}^n : f_i(x) = 0\}. \tag{5}$$

The next proposition characterizes the basic dynamic behavior of CTLN models.

Proposition 1. *Given the system (1), suppose it has a connectivity matrix W with negative entries and an input $b \in \mathbb{R}^n$ with positive coordinates. Define $B = \prod_{i=1}^n [0, b_i]$ and let $x_0 \in \mathbb{R}^n$ be an initial condition, then:*

- (i) *If $x_0 \in B$, the solution $x(t)$ is bounded.*
- (ii) *For $t > 0$ we have $x(t) \in B$.*
- (iii) *Let x^* be an equilibrium point, so $x^* \in B$.*

Proof

- (i) As $\dot{x}_i + x_i = [W_i x + b_i]_+$ we have $(e^t x_i)' = e^t [W_i x + b_i]_+$. Integrating we obtain

$$x_i(t) = e^{-t} \left(\int_0^t e^s [W_i x(s) + b_i]_+ ds + x_i(0) \right). \tag{6}$$

From the last equation follows $x_i(t) \geq e^{-t} x_i(0) \geq 0$. So, we obtain $\sum W_{ik} x_k \leq 0$, then $[W_i x + b_i]_+ \leq b_i$. Finally, we conclude $x_i(t) \leq e^{-t} (b_i e^t - b_i + x_i(0))$.

- (ii) Follows from the two inequalities obtained in the previous item.
- (iii) Necessary to hold $x_i^* = [W_i x + b_i]_+ \geq 0$. Then $\sum W_{ik} x_k \leq 0$, we conclude $x_i^* = [W_i x + b_i]_+ \leq b_i$. ■

Remark 2.1. From the previous proposition, the box B determined by the input $b \in \mathbb{R}^n$ is a natural scenario to search for possible homoclinic or heteroclinic connections. That is why we restrict our numerical simulations to that region of space.

Remark 2.2. If P is a permutation matrix that commutes with W and the input b has equal components, then the application $x \rightarrow Px$ is an automorphism of system.

Given a CTLN with connectivity matrix W , we can construct a directed graph G_W with the rule

$$G_W \text{ has an edge } j \rightarrow i \Leftrightarrow W_{ij} > -1. \tag{7}$$

In [Morrison *et al.*, 2016], the authors consider only competitive networks with only two values for the connections: one fixed value for $W_{ij} < -1$, and another for $W_{ij} > -1$. So, to any simple directed graph G of n vertices and for any $0 < \epsilon < 1$ and $\delta > 0$, they associate a corresponding $n \times n$ connectivity matrix $W = W(G, \epsilon, \delta)$ as follows:

$$W_{ij} = \begin{cases} 0 & \text{if } i = j \\ -1 + \epsilon & \text{if } j \rightarrow i \\ -1 - \delta & \text{if } j \nrightarrow i. \end{cases} \tag{8}$$

Clearly, $G_W = G$. Finally, for every $b \in \mathbb{R}^n$ with positive coordinates and given a simple directed graph G , we get a CTLN.

3. The Modified Case

Given a simple directed graph G of n nodes, we proceed in an analogous way to (8) and define a threshold linear network as follows: Fix $\alpha > 0$, $0 < \epsilon < \alpha$ and $\delta > 0$, we take

$$W_{ij} = \begin{cases} 0 & \text{if } i = j \\ -\alpha + \epsilon & \text{if } j \rightarrow i \\ -\alpha - \delta & \text{if } j \nrightarrow i. \end{cases} \tag{9}$$

Building the network in this way, we can continue classifying inhibitory connections into strong and weak, differentiating them by $W_{ij} < -\alpha$ or $W_{ij} > -\alpha$ respectively, where α is an arbitrary threshold for comparing inhibitions. This leaves aside the classification obtained by comparing with self-inhibition (although this scenario recovers for $\alpha = 1$). We study the case when the inhibition of each node overcomes self-inhibition. For this, we

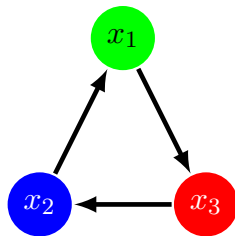


Fig. 1. Oriented graph.

just take $\alpha > 1 + \epsilon$. Consider the complete graph of three nodes, oriented clockwise. In that case, the connectivity matrix has the form

$$W = \begin{pmatrix} 0 & -\alpha - \delta & -\alpha + \epsilon \\ -\alpha + \epsilon & 0 & -\alpha - \delta \\ -\alpha - \delta & -\alpha + \epsilon & 0 \end{pmatrix}. \quad (10)$$

Given $\lambda > 0$ consider the CTLN with connectivity matrix W and input $b = (\lambda, \lambda, \lambda)$. Notice that the connectivity matrix commutes with permutation matrices P_{312} and P_{231} . It is thus defined an action of \mathbb{Z}_3 over the system (cf. Remark 2.2). We write eq_i as the equilibrium point for the sector S_i . If $\alpha > 1 + \epsilon$ the seven possible equilibria coexist. Also, it is easy to check

$$\lim_{\alpha \rightarrow 1+\epsilon} eq_1 = eq_{31}. \quad (11)$$

Analogously $eq_2 \rightarrow eq_{12}$ and $eq_3 \rightarrow eq_{23}$. It must be noted that $eq_{12} \in \Sigma_3$, $eq_{31} \in \Sigma_2$ and $eq_{23} \in \Sigma_1$ if $\alpha > 1 + \epsilon$, and they are stables nodes (*permitted sets*, in the nomenclature of [Curto *et al.*, 2012] and [Curto *et al.*, 2013]). When $\alpha = 1 + \epsilon$, the equilibrium eq_j collides with eq_{ij} , and both disappear for $\alpha < 1 + \epsilon$. The only equilibrium point that persists in all scenarios is eq_0 .

Remark 3.1. Note all unstable equilibria of new system are inside the box $B = [0, \lambda]^3$. So, applying Proposition 1 it follows that all possible homoclinic or heteroclinic connections can only be inside the box B .

Remark 3.2. For some values $\alpha > 1 + \epsilon$ we find heteroclinic cycles. In such cycles, eq_0 is connected to all other equilibrium points. For other values $\alpha > 1 + \epsilon$, we only find a stable limit cycle. We conjecture that there is a value $\alpha_0 > 1 + \epsilon$ such that heteroclinic cycles exist for $\alpha \geq \alpha_0$. In the opposite case, there is a limit cycle and only isolated heteroclinic connections remain.

Recall that restricted to a sector S_i or S_{ij} the system is linear. Then, if there is an equilibrium in the sector S_i or S_{ij} , its stable and unstable manifolds will be linear varieties inside the region, we write \mathcal{W}_i^s or \mathcal{W}_i^u for those varieties. In particular, if $n = 3$, we have stable/unstable planes or lines. We write N_i (N_{ij}) the principal matrix of restricted system. In addition, we can consider $\lambda = 1$ without loss of generality.

3.1. The limit cycle

The limit cycle appears for $\alpha < \alpha_0$ and remains for $\alpha < 1 + \epsilon$, it contracts until $\alpha = 1 + \frac{(\epsilon - \delta)}{2}$, for this value eq_0 becomes an unstable center. In the case $\alpha = 1$, we obtain the cycle reported in [Morrison *et al.*, 2016]. The cycle is counterclockwise, and we have the next itinerary (crossing the corresponding transition varieties):

$$S_{12} \xrightarrow{\Sigma_1} S_2 \xrightarrow{\Sigma_3} S_{23} \xrightarrow{\Sigma_2} S_3 \xrightarrow{\Sigma_1} S_{31} \xrightarrow{\Sigma_3} S_1 \xrightarrow{\Sigma_2} S_{12}. \quad (12)$$

Notice that the cycle is an invariant set by the permutations, P_{231} rotates it clockwise and P_{312} counterclockwise.

3.2. The heteroclinic cycles

In this section, we make a description of the heteroclinic cycles (based on numerical simulations), and show the *twisting effect*, that is proved in the next section. When the critical value α_0 is exceeded, we observe the appearance of an heteroclinic cycle, represented in Fig. 4, composed by connections between the eq_i with the eq_{ij} equilibria (solid and simple dotted lines), and infinite connections between eq_0 and the eq_{ij} (double dotted lines). The shown figure is valid for α not so close to critical value α_0 . Let it be pointed out that the solid connections are robust and exist for all $\alpha > 1 + \epsilon$, meanwhile the dotted lines suffer a *twisting effect* when $\alpha \rightarrow \alpha_0$. This effect we will describe in the last subsection.

3.2.1. Connections of eq_i with eq_{ki}

Consider the solid connections as in Fig. 4. Take for example, the connection of eq_2 with eq_{12} inside the sector S_2 , the equilibrium eq_2 has $u_2 = \left(-\frac{\sqrt{(\alpha+\delta)(\alpha-\epsilon)}}{\alpha+\delta}, 0, 1\right)$ as unstable direction. So we

Table 1. Equilibria of system.

Sector	Equilibrium	Unstability	Type
S_0	$eq_0 = \left(\frac{\lambda}{(1+2\alpha+\delta-\epsilon)}, \frac{\lambda}{(1+2\alpha+\delta-\epsilon)}, \frac{\lambda}{(1+2\alpha+\delta-\epsilon)} \right)$	2	Focus
S_1	$eq_1 = \left(0, \frac{\lambda(\alpha+\delta-1)}{\alpha^2+\alpha(\delta-\epsilon)-\delta\epsilon-1}, \frac{\lambda(\alpha-\epsilon-1)}{\alpha^2+\alpha(\delta-\epsilon)-\delta\epsilon-1} \right)$	1	Saddle
S_2	$eq_2 = \left(\frac{\lambda(\alpha-\epsilon-1)}{\alpha^2+\alpha(\delta-\epsilon)-\delta\epsilon-1}, 0, \frac{\lambda(\alpha+\delta-1)}{\alpha^2+\alpha(\delta-\epsilon)-\delta\epsilon-1} \right)$	1	Saddle
S_3	$eq_3 = \left(\frac{\lambda(\alpha+\delta-1)}{\alpha^2+\alpha(\delta-\epsilon)-\delta\epsilon-1}, \frac{\lambda(\alpha-\epsilon-1)}{\alpha^2+\alpha(\delta-\epsilon)-\delta\epsilon-1}, 0 \right)$	1	Saddle
S_{12}	$eq_{12} = (0, 0, \lambda)$	0	Node
S_{23}	$eq_{23} = (\lambda, 0, 0)$	0	Node
S_{31}	$eq_{31} = (0, \lambda, 0)$	0	Node

have the next parametrization of the invariant manifold (inside the sector):

$$\mathcal{W}_2^u = tu_2 + eq_2. \tag{13}$$

If $t > 0$, the line points to the transition variety Σ_1 and cuts it at a single point q . From there, the trajectory stays inside the sector S_{12} , where the equilibrium eq_{12} is globally stable. So the heteroclinic connection appears. The connections $eq_1 \rightarrow eq_{31}$ and $eq_3 \rightarrow eq_{23}$ follow from the invariance of the system under the permutations P_{231} and P_{312}

respectively. Note that each of these connections exist for $\alpha > 1 + \epsilon$.

3.2.2. Connections of eq_0 with eq_i

The existence of dotted black connections of Fig. 4 are suggested by Fig. 6. Note that as we approach the boundaries between color regions, the heteroclinic connections with origin from eq_0 are getting closer to the eq_i equilibria. From this, the connections coincide with the boundaries.

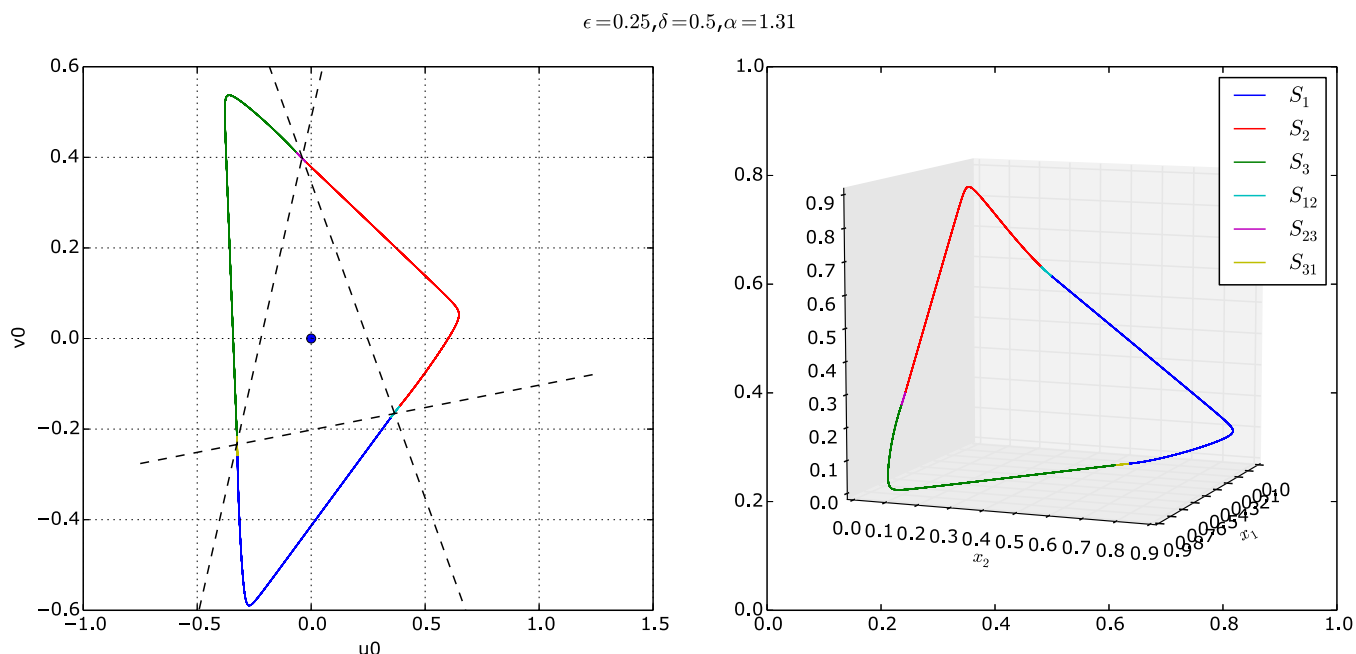


Fig. 2. Projected limit cycle over the unstable plane of eq_0 and 3D view.

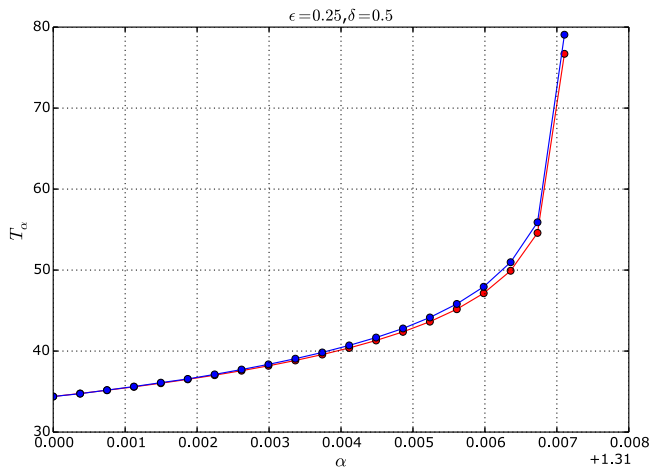


Fig. 3. Blue curve: Growth of periods of the cycles as α approaches the critical value α_0 from below. Red curve: function $6.95 \log \left(\frac{1}{\alpha - \alpha_0} \right)$ ($\alpha_0 \approx 1.31712123845$).

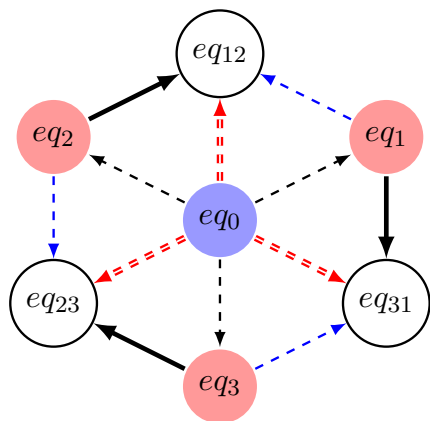


Fig. 4. Scheme of heteroclinic cycle from values of α not so close to α_0 .

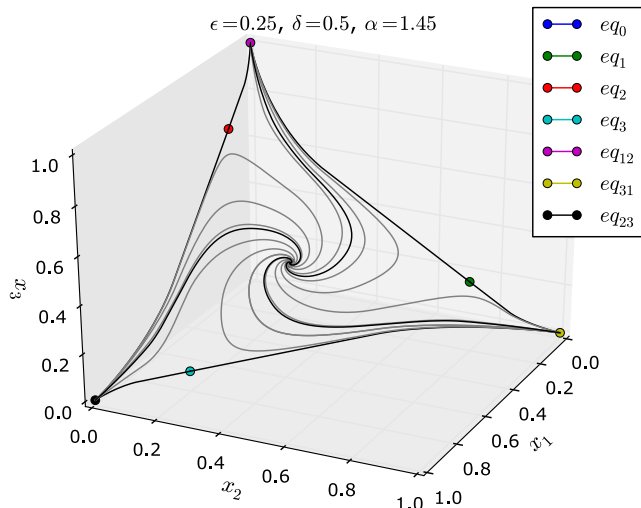


Fig. 5. Heteroclinic cycle, 3D view.

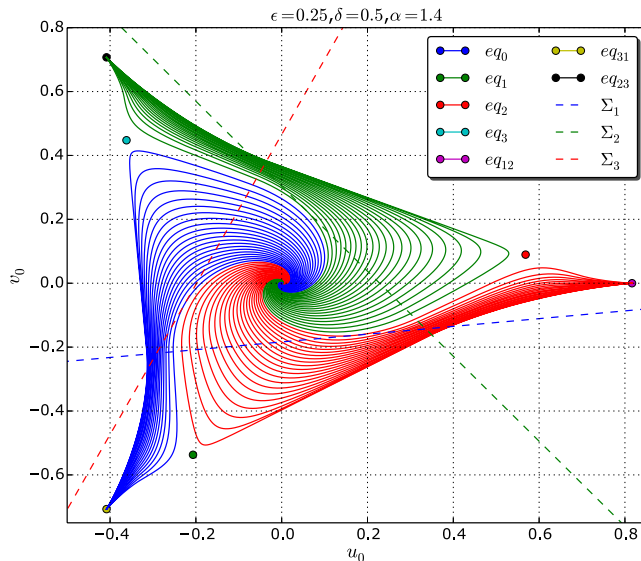


Fig. 6. Projection of heteroclinic cycle over the unstable plane of eq_0 . The axes u_0 and v_0 corresponding to the principal unstable directions. The dotted lines mark the intersection with the transition planes.

3.2.3. The other connections

The other connections (cf. Fig. 4) of the eq_i with the eq_{ik} (the blue lines), and the connections of eq_0 with the eq_{ij} (red lines) were obtained numerically. We remark that its simulations are easier than the previous commented connections.

3.2.4. The twisting effect

Figures 8 to 10 are organized by decreasing values of parameter α and simulating the dotted connection of Fig. 4 with origin in eq_2 (the other heteroclinic

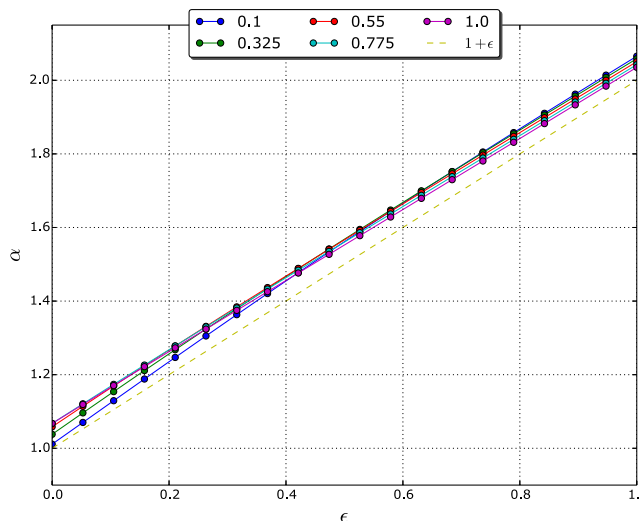


Fig. 7. Bifurcation curves of ϵ versus α (δ fixed).

$\epsilon = 0.25, \delta = 0.5, \alpha = 1.33$

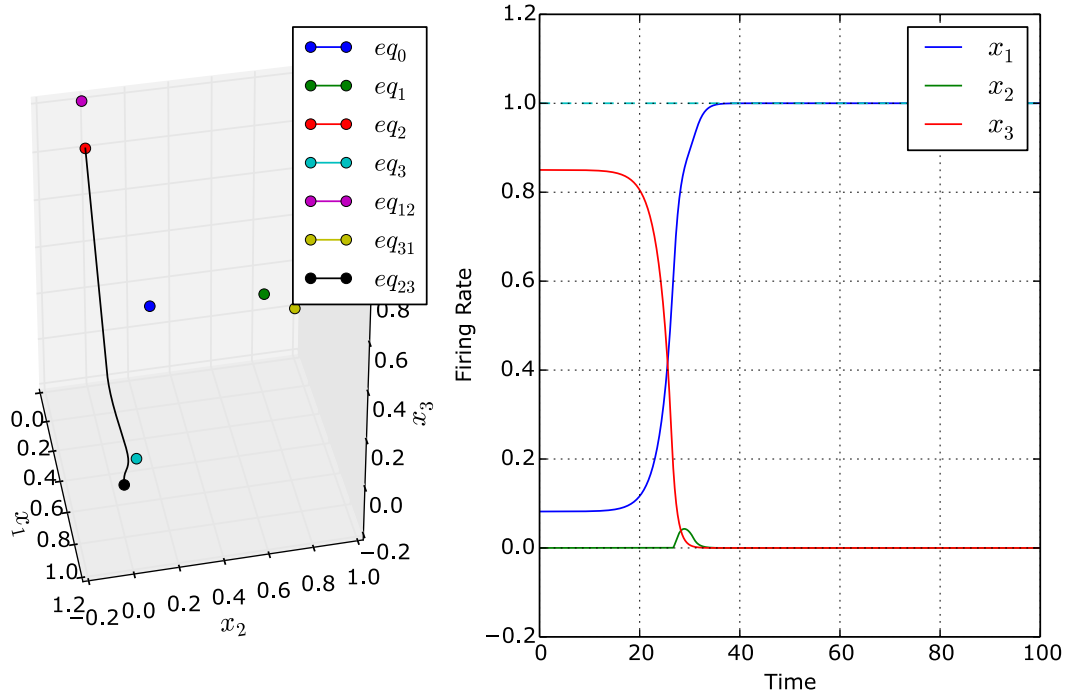


Fig. 8. Simple heteroclinic connection between eq_2 and eq_{23} .

$\epsilon = 0.25, \delta = 0.5, \alpha = 1.31712123756$

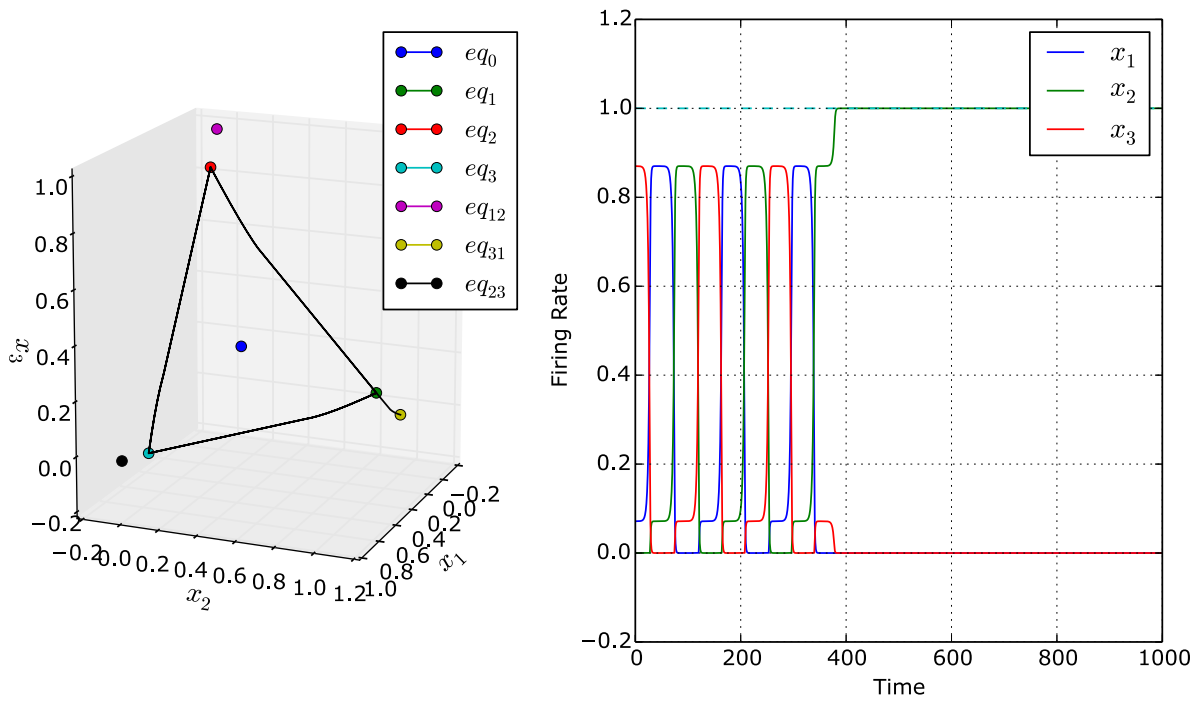


Fig. 9. Twisted heteroclinic connection between eq_2 and eq_{31} .

$$\epsilon = 0.25, \delta = 0.5, \alpha = 1.31712123755$$

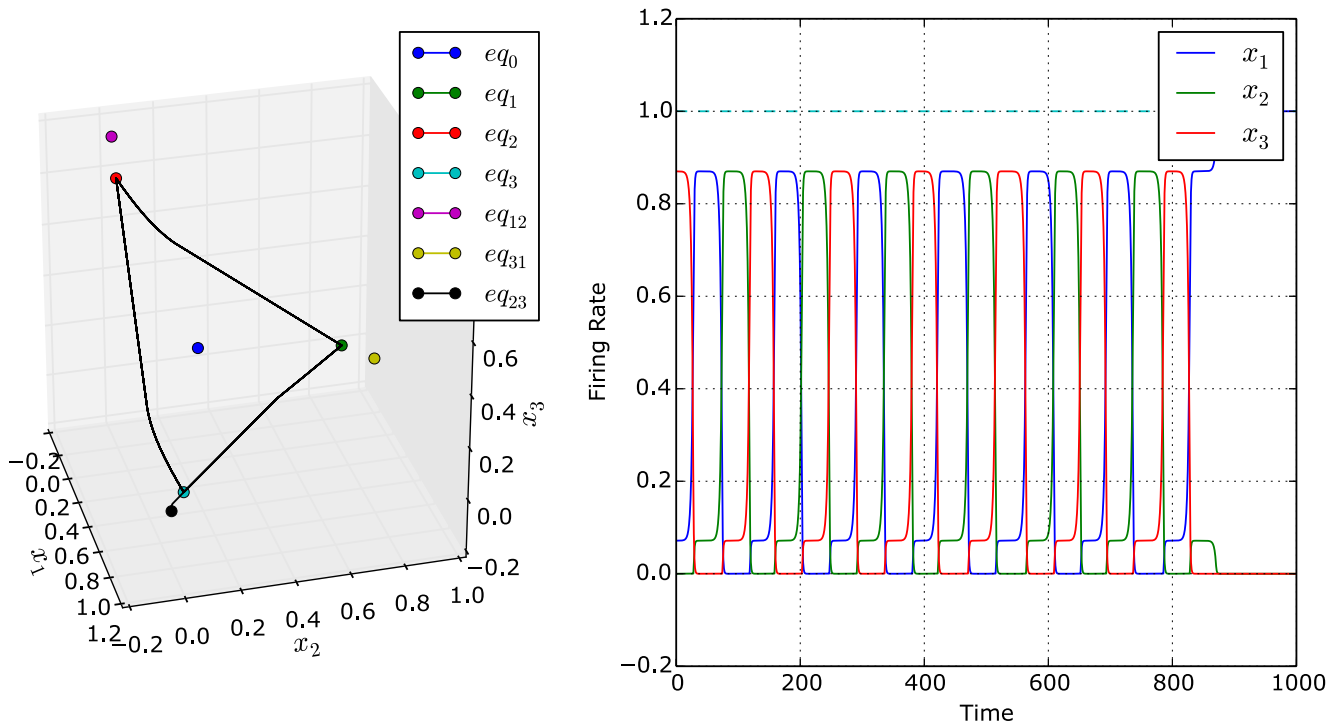


Fig. 10. Twisted heteroclinic connection between eq_2 and eq_{23} .

connections with origin in eq_1 and eq_3 have similar behavior by symmetry of the system). It can be observed that for values of α near α_0 (in this case, we estimate $\alpha_0 = 1.31712123845$ for $\epsilon = 0.25$ and $\delta = 0.5$), the connections twist around the triangle formed by the equilibria eq_1, eq_2, eq_3 and change its final equilibria and new cycles are created (represented in Figs. 13 and 12). In Fig. 11 the orbits are *unwound* by adding a positive and growing function to calculated solution (also the equilibria has an adequate shift). We must remark that near the critical value α_0 the simulations have high levels of numerical error. Based on the simulations, we conjecture the next theorem:

Theorem 1 [Twisting Effect]. *Given $\rho > 0$ and $n \in \mathbb{N}$, there exists a value $\alpha = \alpha(\rho, n) > \alpha_0$ and an heteroclinic orbit that connects eq_k ($k = 1, 2, 3$) with some node eq_{ij} or saddle eq_i and crosses n times the transition varieties Σ_j .*

In Figs. 14–16, it can be observed the twisting effect for connections with origin in eq_0 , and parameter values $\epsilon = 0.15$, $\delta = 0.5$ and an estimated critical

value $\alpha_0 = 1.2139083785$. By this twisting effect, the connections that begin from eq_i change to its final equilibrium as the parameter α varies. This produces a cascade of bifurcations near the critical value α_0 .

3.3. Analysis of saddle connections

Now we make a convenient transformation of coordinates to study the system. We take the transition varieties as the coordinate planes. Thus the regions will coincide with the quadrants. So, we take the affine transformation

$$x \mapsto z = Wx + b. \tag{14}$$

In the new coordinates the system will have the form

$$\dot{z} = -z + b + W[z]_+. \tag{15}$$

3.3.1. Connection between eq_i and eq_{ji}

Denote with $\Sigma_i^- = \{z_i = 0, z_{(i+1 \bmod 3)} < 0\}$ and consider without loss of generality the equilibrium eq_1 . We denote with Γ_α the branch of the unstable

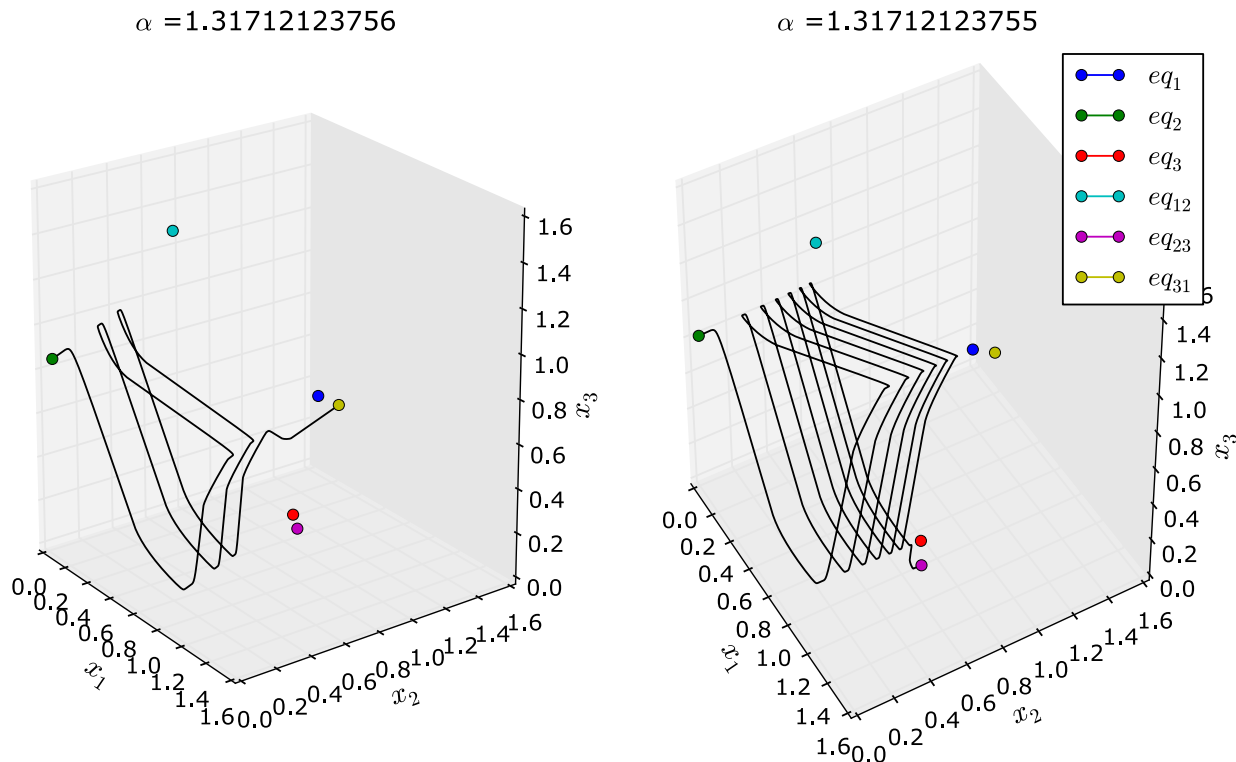


Fig. 11. Solution + $\frac{\sqrt{t}}{700}(1, 1, 1)$.

manifold of eq_1 that points in the opposite direction to the equilibrium eq_{31} . We take $\alpha = 1 + 2\epsilon$. For such value of the parameter, by simulation we obtain that eq_1 is connected to the equilibrium eq_{12} . Then $\Gamma_{\alpha=1+2\epsilon}$ is an heteroclinic connection, beginning in the region S_1 and ending in S_{12} . Therefore, in this situation, the trajectory must intersect the variety Σ_2 .

We observe (by simulation, again) that the following occurs (see Fig. 18): there exist values $\beta < \alpha_0 < \alpha^* < 1 + 2\epsilon$ for which, if $\alpha \in (\alpha^*, \infty)$ the trajectory Γ_α crosses Σ_2 and reaches equilibrium eq_{12} . On the other hand, if $\alpha \in (\beta, \alpha^*)$, we have that Γ_α (whether it is an heteroclinic connection or not), first intersects Σ_2 and then Σ_1 , entering in the region S_2 .

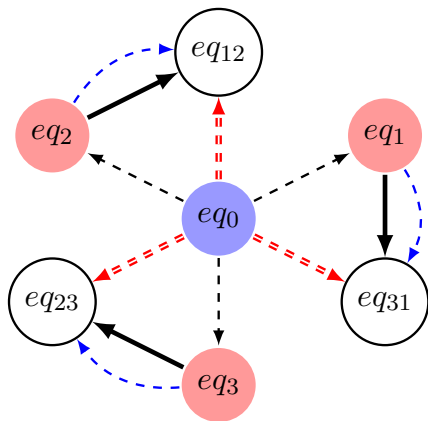


Fig. 12. Scheme of new heteroclinic cycle that appears from values of α so close to α_0 .

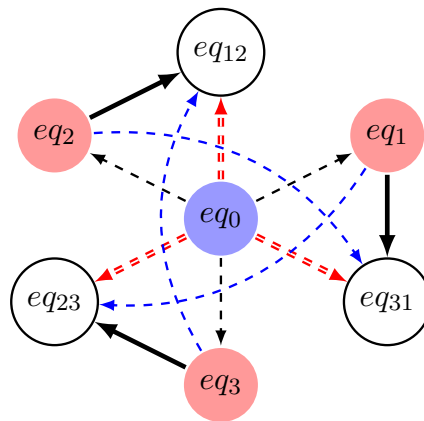


Fig. 13. Scheme of new heteroclinic cycle that appears from values of α so close to α_0 .

$$\epsilon = 0.15, \delta = 0.5, \alpha = 1.21391$$

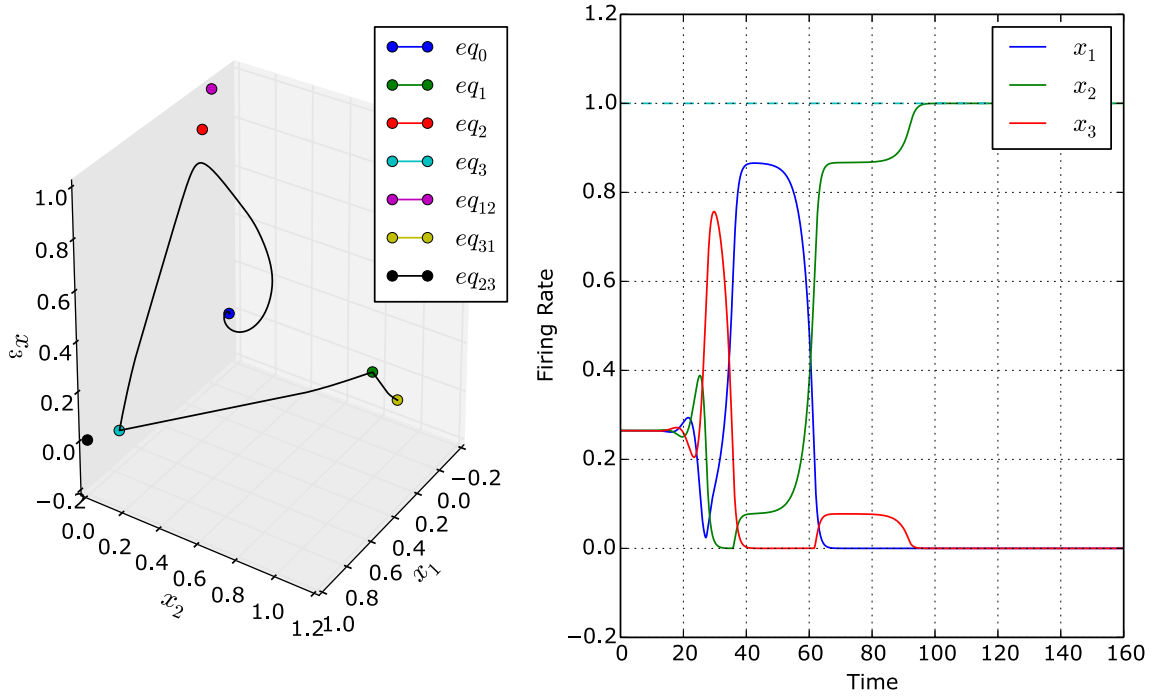


Fig. 14. Heteroclinic connections between eq_0 and eq_{31} .

$$\epsilon = 0.15, \delta = 0.5, \alpha = 1.213908379$$

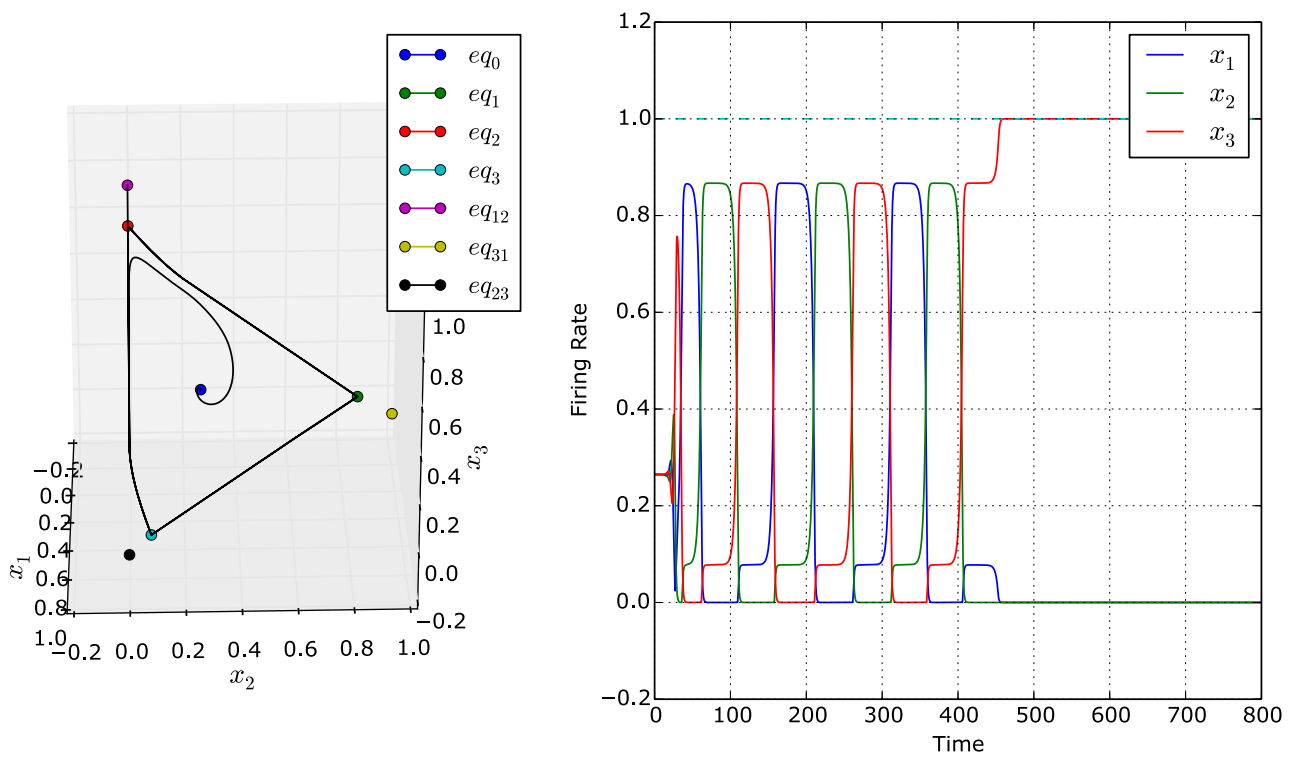


Fig. 15. Heteroclinic connections between eq_0 and eq_{12} .

$$\epsilon = 0.15, \delta = 0.5, \alpha = 1.2139083786$$

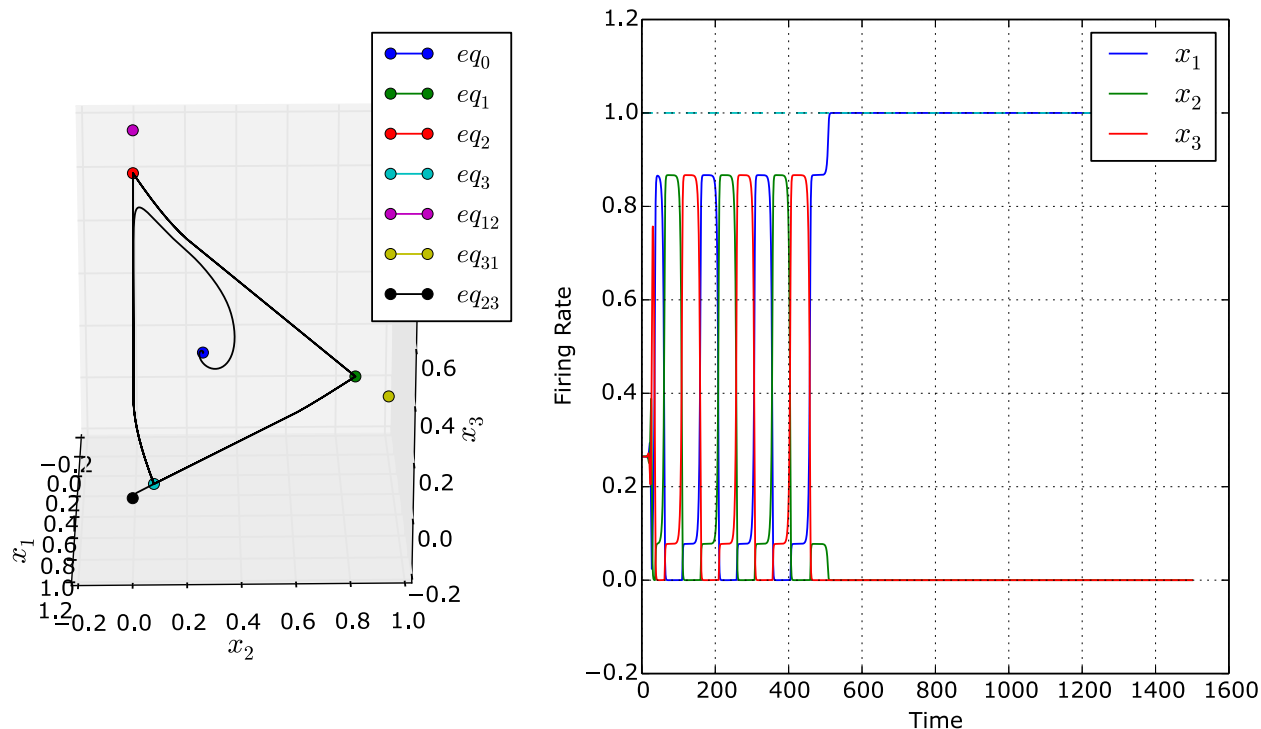


Fig. 16. Heteroclinic connections between eq_0 and eq_{23} .

Consider $\alpha < \alpha^*$. Let $Q_\alpha^1 \in \Gamma_\alpha \cap \Sigma_1^-$ be the point where the trajectory first cuts across the transition variety Σ_1 . If Q_α^1 is above the stable plane of eq_2 (dotted line of Fig. 19), then the trajectory will approach such an equilibrium but finally it will be captured by the unstable direction (red dashed line) and drops to the stable node eq_{12} .

If $Q_\alpha^1 \in \mathcal{W}_2^s$, i.e. it is inside the stable plane of eq_2 , the trajectory ends in eq_2 and we have a saddle connection of codimension-1.

Finally, if Q_α^1 is below the stable plane of eq_2 , the trajectory will approach such an equilibrium, and will be captured by the unstable direction and continues in that direction. See Fig. 20.

3.3.2. Heteroclinic and homoclinic bifurcations

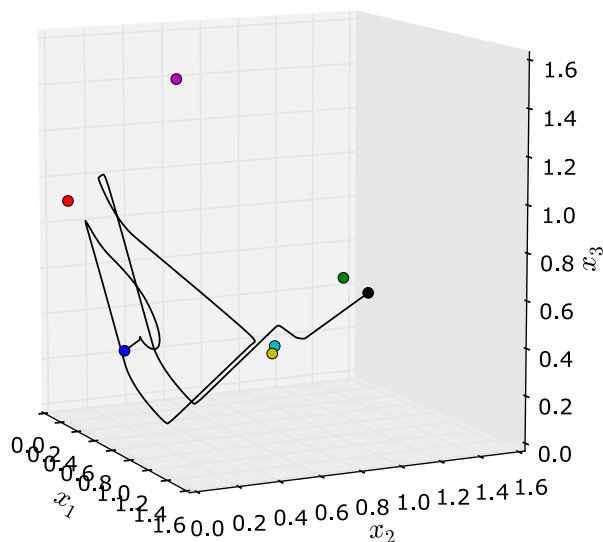
Starting from the last case described in the previous section we consider the diagram shown in Fig. 21, so the point Q_α^1 is below the $\mathcal{W}_2^s \cap \{z_2 = 0\}$. Then the trajectory dragged by the unstable equilibrium direction eq_2 continues and cuts across the plane $\Sigma_3 = \{z_3 = 0\}$ and then cuts the half-plane Σ_2^- , where it interacts with the stable manifold

\mathcal{W}_3^s . Then we obtain similar scenarios to the previous section as the new point Q_α^2 is found above, below or in $\mathcal{W}_3^s \cap \Sigma_3$. In this way it may happen that:

- (a) Q_α^2 cuts above the stable manifold of eq_3 and there emerges a heteroclinic connection with eq_{23} .
- (b) Q_α^2 cuts the plane Σ_2^- coinciding with the stable manifold of eq_3 and there emerges a connection between the saddles eq_1 and eq_3 .
- (c) Q_α^2 cuts below the stable plane eq_3 , so the trajectory is dragged by the unstable direction of eq_3 and continues. Finally it cuts Σ_1 and Σ_3^- .

In the latter case, the trajectory initiated in eq_1 must interact with the stable manifold of eq_1 . Then again, if the cut point of the trajectory and Σ_3^- is above the stable manifold, there is a new connection with the node eq_{31} , then there will be a double heteroclinic connection between eq_1 and eq_{31} . But if the cut point Q_α^3 of the trajectory with the Σ_3^- plane lies on the stable manifold, we will have a *homoclinic connection*. Such homoclinic connection

$\alpha = 1.213908379$



$\alpha = 1.2139083786$

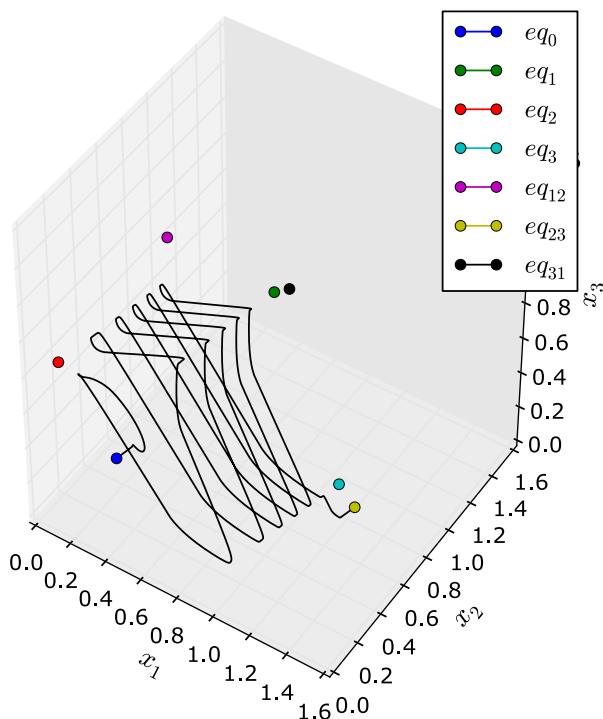


Fig. 17. Solution $+ \frac{(\exp(-t)+1)\sqrt{I}}{700}(1, 1, 1)$.

will be broken when the parameter α varies and the point Q_α^3 is below the intersection $\mathcal{W}_1^s \cap \{z_3 = 0\}$ and continues being dragged in the unstable direction. From there it continues to cut the variety Σ_2 and then Σ_1^- at a point Q_α^4 that can be above,

below or over the intersection $\mathcal{W}_2^s \cap \{z_1 = 0\}$. Thus there is a *twisting effect* of the trajectory which initiates in eq_i which gives rise to heteroclinic and homoclinic bifurcations as we approach the critical value α_0 .

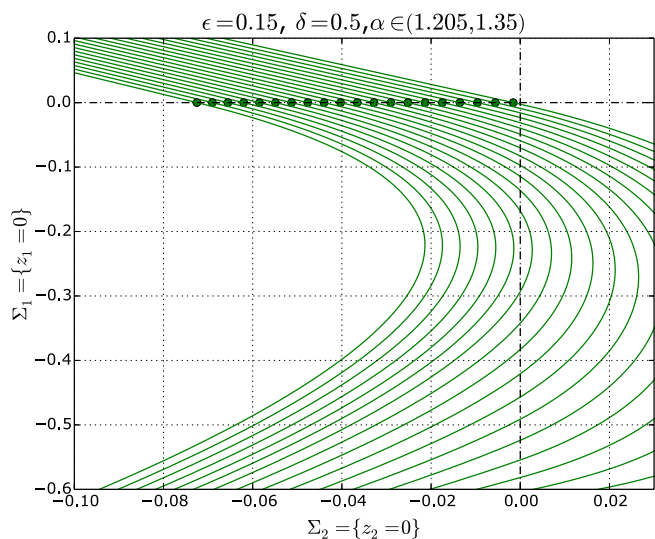


Fig. 18. The green points show the location of the first point of intersection between Γ_α and Σ_2 , for different values of α . They shift from left to right as the value of α decreases.

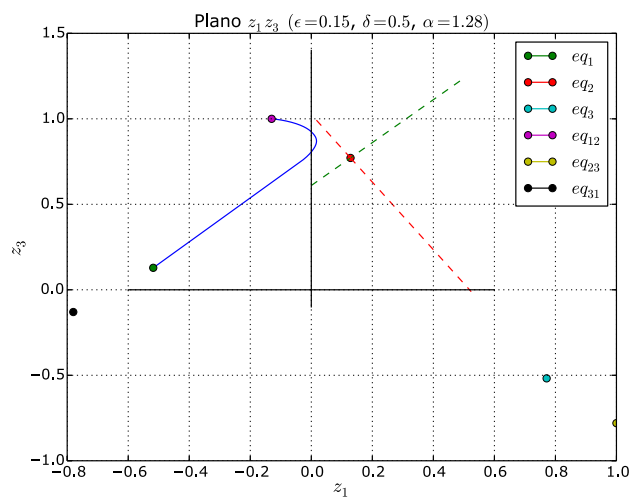


Fig. 19. The trajectory cuts over the stable plane of eq_2 and there emerges a heteroclinic connection. The green dashed line is the stable plane of eq_2 , the red dashed line the unstable direction.

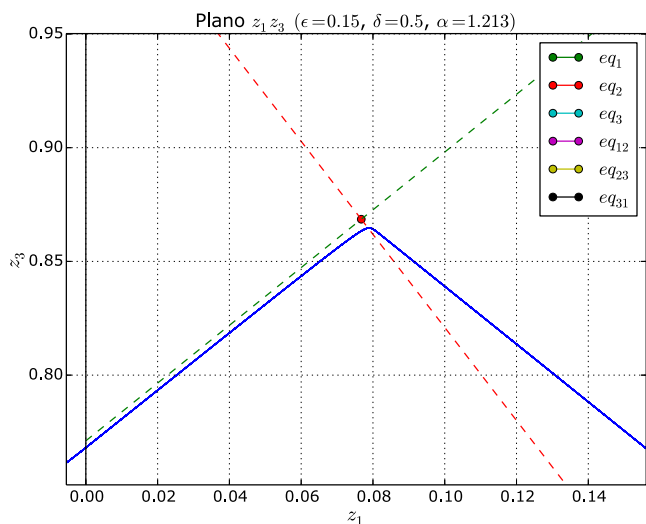


Fig. 20. The trajectory cuts below the stable plane of eq_2 .

3.4. The main result

Consider the next version of Theorem 1.

Theorem 2. *Let us take, without loss of generality, the heteroclinic Γ_α with origin in eq_1 and that points in the opposite direction to the node eq_{31} . Then, there exist infinite values $\alpha > \alpha_0$ such that Γ_α ends in any of the equilibria (except eq_0) and cuts across as many times as we want the transition variety Σ_1^- (this is called twisting effect).*

In order to prove the above result, we continue with the same method developed in the previous subsection. We can define Q_α^i as the cut point of the trajectory with the corresponding variety each time

that the trajectory interacts with the stable plane of some equilibrium by cutting the half-plane Σ_j^- . Then we have

$$Q_\alpha^i \in \Sigma_{(i \bmod 3)}^- \tag{16}$$

By construction, if there exists $Q_{\alpha_i}^i$, and $i = 3k + l$ where $l \equiv i \pmod 3$, then the trajectory has traversed $k + 1$ times the half-plane Σ_i^- . Therefore, the proof of Theorem 2 is reduced to find conditions for which Q_α^i is well defined.

On the other hand, we have that the resulting line of the intersection $\mathcal{W}_{(i+1 \bmod 3)}^s \cap \Sigma_i^-$ is always constant in the component $z_{(i+1 \bmod 3)}$, and since z_i is zero, it follows that the position of the point Q_α^i with respect to the stable plane will depend only on the component $z_{(i+2 \bmod 3)}$. To see this, we just take the stable directions $u_{(i+1 \bmod 3)}$ and $v_{(i+1 \bmod 3)}$ corresponding to $eq_{(i+1 \bmod 3)}$ and note that the normal vector to the stable plane, $w_{(i+1 \bmod 3)} = u_{(i+1 \bmod 3)} \times v_{(i+1 \bmod 3)}$, satisfies that its component $(i + 1 \bmod 3)$ is null. In other words, we will have

$$\begin{aligned} \mathcal{W}_{(i+1 \bmod 3)}^s \cap \Sigma_i^- \\ = \{z_i = 0, z_{(i+2 \bmod 3)} = C_\alpha, z_{(i+1 \bmod 3)} < 0\} \end{aligned} \tag{17}$$

where

$$C_\alpha = \frac{\langle w_{(i+1 \bmod 3)}; eq_i \rangle}{\langle w_{(i+1 \bmod 3)}; e_{(i+2 \bmod 3)} \rangle}. \tag{18}$$

Note that for all i the value of $C_\alpha > 0$ is the same by symmetry. Given the point $Q_\alpha^i \in \Sigma_{(i \bmod 3)}^-$ where

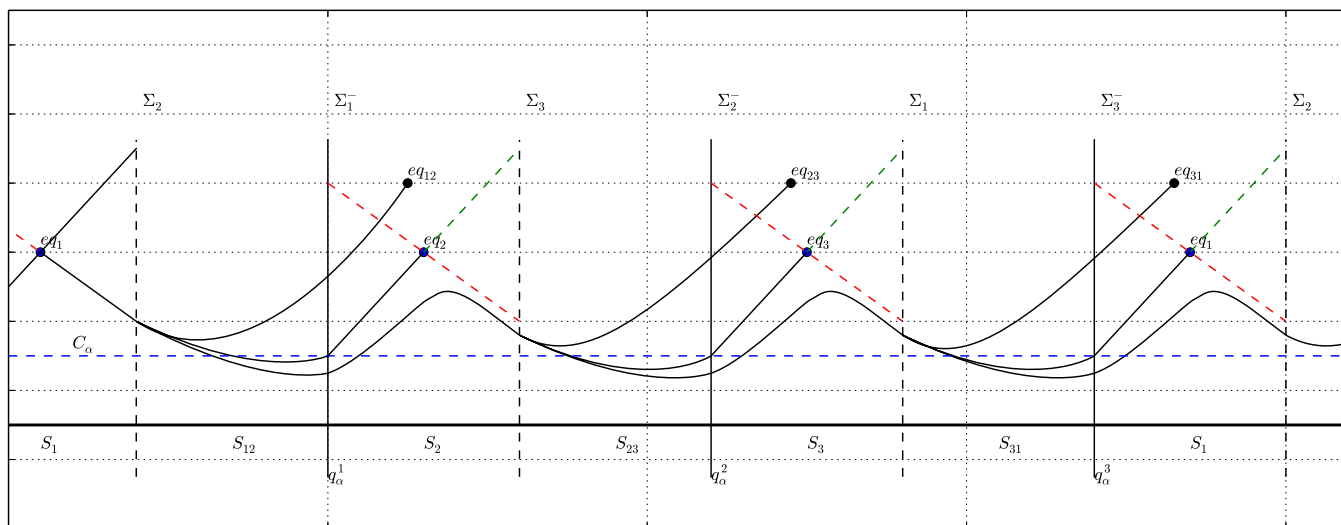


Fig. 21. Schematic diagram of possible trajectories. When you cut some Σ_i^- there are three possible cutting heights, and depending on that, different connections are born or the trajectory continues.

the trajectory Γ_α interacts with the stable manifold of $eq_{(i+1 \bmod 3)}$, write as q_α^i the value of its component that determines if the point Q_α^i is above, below or inside of $W_{(i+1 \bmod 3)}^s$, i.e.

$$q_\alpha^i = \langle e_{(i+1 \bmod 3)}, Q_\alpha^i \rangle. \tag{19}$$

3.4.1. The q_α^i family

As stated above we have functions q_α^i . It is immediate that given α the value q_α^{i+1} is defined if and only if $q_\alpha^i < C_\alpha$. Besides, it must happen that:

$$\text{Dom}(q_\alpha^{i+1}) \subset \text{Dom}(q_\alpha^i). \tag{20}$$

The continuity of the functions q_α^i with respect to the parameter α follows from the continuity of solutions of system (15) with respect to the parameter.

By construction of q_α^i follows immediately the next result:

Theorem 3. *Given the family q_α^i , take a value $\alpha \in (\beta, \infty)$. Then*

- (i) *there is an heteroclinic connection between eq_1 and $eq_{(i \bmod 3, i+1 \bmod 3)}$ iff $q_\alpha^i > C_\alpha$.*
- (ii) *there is a saddle connection eq_1 and $eq_{(i+1 \bmod 3)}$ iff $q_\alpha^i = C_\alpha$. In particular, if $i + 1 \equiv 0 \bmod 3$ there is an homoclinic connection.*
- (iii) *the trajectory tends to a stable limit cycle iff q_α^i is defined for all $i \in \mathbb{N}$. Necessarily it holds $q_\alpha^i < C_\alpha$ and, in particular, $\alpha < \alpha_0$.*

Proof. The first two items are immediate. In the third, the right implication is immediate. The left implication follows from the fact that there are no other possible attractors (or at least, they have not been found by simulation). ■

In the next, we propose two hypotheses that guarantee a regular behavior of the family $\{q_\alpha^i\}$. Such hypotheses postulate the monotonous growing of the functions and they make it possible to determine the sign of q_α^i when the function is defined.

Hypothesis 1 [H1]. *Suppose $q_\alpha^i - C_\alpha$ is increasing monotonically. So, if $q_\alpha^{(i+1)}$ exists then it is increasing monotonically too.*

Hypothesis 2 [H2]. *Given $i \in \mathbb{N}$ exists, $\delta = \delta(i)$ such that, if $0 < C_\alpha - q_\alpha^i < \delta$ then $q_\alpha^{(i+1)} > C_\alpha$.*

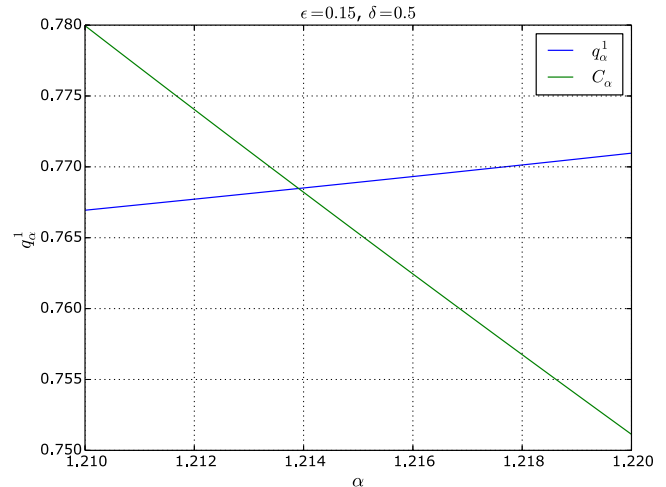


Fig. 22. The blue curve shows the monotonous function q_α^1 .

Proposition 2. *Suppose the validity of H1 and H2. Then*

$$\text{Dom}(q_\alpha^i) = (\beta, \alpha_i) \tag{21}$$

where α_i is such that $q_{\alpha_i}^{(i-1)} - C_{\alpha_i} = 0$.

Proof. We proceed by induction. Let us first observe that $q_\alpha^1 - C_\alpha$ is increasing monotonically (see Fig. 22). And we observe that $\text{Dom}(q_\alpha^1) = (\beta, \alpha_1)$. Then, by induction (using H1) it follows that, if it is defined, $q_\alpha^i - C_\alpha$ will be increasing monotonically.

Suppose that $\text{Dom}(q_\alpha^i) = (\beta, \alpha_i)$. As $C_{\alpha_i} = q_{\alpha_i}^{(i-1)}$, by H2 γ exists such that given $\gamma < \alpha < \alpha_i$, $q_\alpha^i > C_\alpha$ follows.

On the other hand, if we take ρ such that $\beta < \rho < \alpha_0$ we have a limit cycle and necessarily it follows $C_\rho > q_\rho^i$. Because q_α^i is increasing monotonically we obtain that there exists a single value $\alpha_{(i+1)}$ such that $q_{\alpha_{(i+1)}}^i = C_{\alpha_{(i+1)}}$. So, $q_\alpha^{(i+1)}$ is defined in $(\beta, \alpha_{(i+1)})$. ■

The next result, immediately, proves the *twisting theorem*.

Lemma 1. *Suppose the validity of H1 and H2, then for all i there exists a value α such that q_α^i is defined.*

Proof. Again we proceed by induction. First note that given $\alpha \in (\beta, \alpha_1)$ always is defined q_α^1 . Then, assuming the existence of q_α^i and repeating the arguments of the proof of Proposition 2, it follows that there exist values such that $q_\alpha^{(i+1)}$ is defined. ■

4. The Coloring Phenomena

Consider $\alpha > \alpha_0$. Each heteroclinic orbit started at eq_0 ends in some of three stable equilibria (except the few orbits that end in eq_i). Choose and assign a color for each equilibria and color with it all heteroclinic connections started on eq_0 according to the final point. Then, if we take a circle contained in the unstable plane not crossing any transition plane, we have colored all circles (because

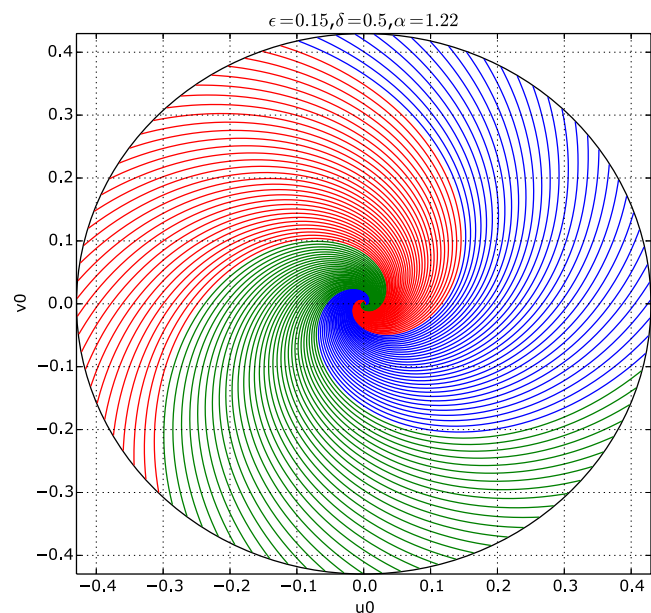


Fig. 23. Coloring phenomena for $\alpha = 1.22$.

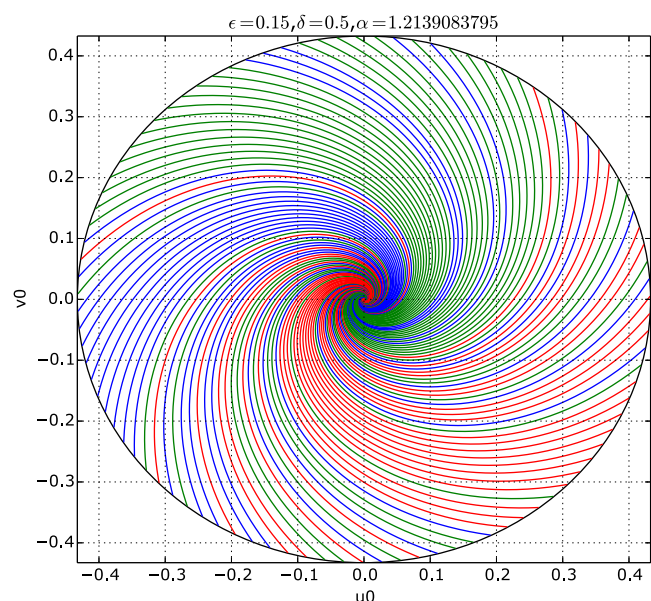


Fig. 24. Coloring phenomena for $\alpha = 1.2139083795$.

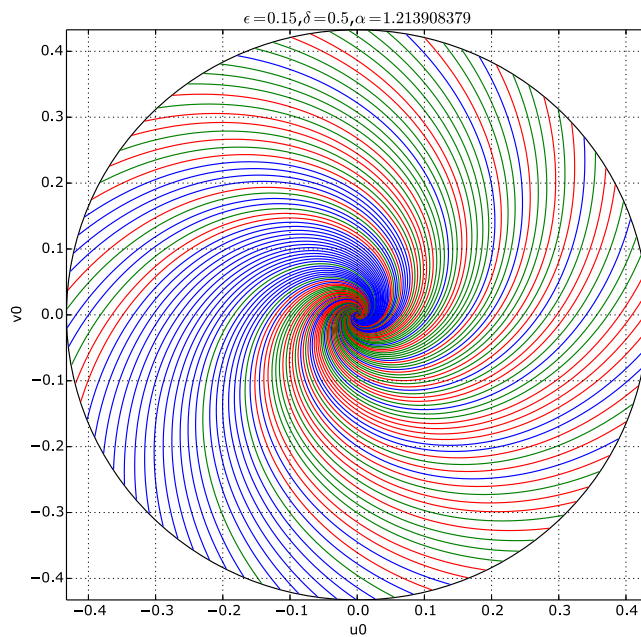


Fig. 25. Coloring phenomena for $\alpha = 1.213908379$.

for any point of the circle, except the center, there is a single heteroclinic). For each value of parameter α we have a particular coloring of the circle. As we approach α_0 the coloring shows complex patterns.

In Figs. 23 to 26 we can see the colorations for α near α_0 . In the figures the colors red, green and blue correspond to the equilibria eq_{12} , eq_{23} and eq_{31} respectively. The connections that end in some eq_i are not captured, that is why a color was not

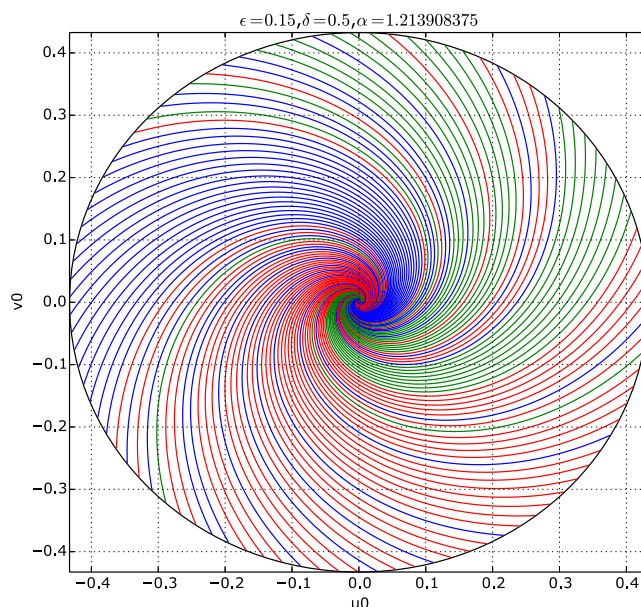


Fig. 26. Coloring phenomena for $\alpha = 1.213908375$.

given. The border between two regions with different colors was formed by an heteroclinic between eq_0 and some eq_i . So, when multiplied the red, green, and blue regions necessarily emerge new connections between eq_0 and the eq_i .

References

- Allesina, S. & Levine, J. [2011] "A competitive network theory of species diversity," *Proc. Natl. Acad. Sci. USA* **108**, 5638–5642.
- Amit, D. [1989] *Modeling Brain Function: The World of Attractor Neural Networks* (Cambridge University Press).
- Curto, C., Degeratu, A. & Itskov, V. [2012] "Flexible memory networks," *Bull. Math. Biol.* **74**, 590–614.
- Curto, C., Degeratu, A. & Itskov, V. [2013] "Encoding binary neural codes in networks of threshold-linear neurons," *Neural Comput.* **25**, 2858–2903.
- Curto, C. & Morrison, K. [2016] "Pattern completion in symmetric threshold-linear networks," *Neural Comput.* **28**, 2825–2852.
- Dai, L. [2008] *Nonlinear Dynamics of Piecewise Constant Systems and Implementation of Piecewise Constant Arguments* (World Scientific, Singapore).
- di Bernardo, M., Budd, C. J., Champneys, A. R. & Kowalczyk, P. [2008] *Piecewise-Smooth Dynamical Systems. Theory and Applications* (Springer-Verlag, NY).
- di Marco, M., Tesi, A. & Forti, M. [2000] "Bifurcations and oscillatory behavior in a class of competitive cellular neural networks," *Int. J. Bifurcation and Chaos* **10**, 1267–1293.
- Grossberg, S. [1988] "Nonlinear neural networks: Principles, mechanisms, and architectures," *Neural Netw.* **1**, 17–61.
- Hahnloser, R. L. T. [1998] "On the piecewise analysis of networks of linear threshold neurons," *Neural Netw.* **11**, 691–697.
- Hahnloser, R. H. R., Seung, H. S. & Slotine, J. J. [2003] "Permitted and forbidden sets in symmetric threshold-linear networks," *Neural Comput.* **15**, 621–638.
- Hirsch, M. W. [1982] "Systems of differential equations which are competitive or cooperative: I. Limit sets," *SIAM J. Math. Anal.* **13**, 167–179.
- Hopfield, J. [1982] "Neural networks and physical systems with emergent collective computational abilities," *Proc. Natl. Acad. Sci. USA* **79**, 2554–2558.
- Itskov, V., Curto, C., Pastalkova, E. & Buzsáki, G. [2011] "Cell assembly sequences arising from spike threshold adaptation keep track of time in the hippocampus," *J. Neurosci.* **31**, 2828–2834.
- Levine, J., Adler, P. & Allesina, S. [2017] "Beyond pairwise mechanisms of species coexistence in complex communities," *Nature* **546**, 56–64.
- Morrison, K., Degeratu, A., Itskov, V. & Curto, C. [2016] "Diversity of emergent dynamics in competitive threshold-linear networks: A preliminary report," arXiv:1605.04463v1 [q-bio.NC].
- Muezzinoglu, M., Tristan, I., Huerta, R., Afraimovich, V. & Rabinovich, M. [2009] "Transients versus attractors in complex networks," *Int. J. Bifurcation and Chaos* **20**, 1653–1675.
- Parmelee, C. [2016] *Applications of Discrete Mathematics for Understanding Dynamics of Synapses and Networks in Neuroscience* (University of Nebraska — Dissertations, Theses, and Student Research Papers in Mathematics), arXiv:1702.06538.
- Rabinovich, M., Volkovskii, A., Lecanda, P., Huerta, R., Abarbanel, H. & Laurent, G. [2001] "Dynamical encoding by networks of competing neuron groups: Winnerless competition," *Phys. Rev. Lett.* **87**, 068102.
- Rabinovich, M., Huerta, R., Varona, P. & Afraimovich, V. [2008] "Transient cognitive dynamics, metastability, and decision making," *PLoS Comput. Biol.* **4**, e1000072.
- Rabinovich, M., Afraimovich, V. & Varona, P. [2014] "Chunking dynamics: Heteroclinics in mind," *Front. Comput. Neurosci.* **8**.
- Rondelez, Y. [2012] "Competition for catalytic resources alters biological network dynamics," *Phys. Rev. Lett.* **108**, 018102.
- Simpson, D. J. W. [2010] *Bifurcations in Piecewise-Smooth Continuous Systems* (World Scientific, Singapore).
- Snoussi, E. [1989] "Qualitative dynamics of piecewise-linear differential equations: A discrete mapping approach," *Dyn. Stab. Syst.* **4**.
- Tang, H. J., Tan, K. C. & Zhang, W. [2005] "Analysis of cyclic dynamics for networks of linear threshold neurons," *Neural Comput.* **17**, 97–114.